Vertical Cavity Surface Emitting Terahertz Laser

A. V. Kavokin,[1] I. A. Shelykh,[2] T. Taylor,[3] and M. M. Glazov[4]

[1]*Spin Optics Laboratory, St. Petersburg State University, 1, Ulianovskaya, 198504, Russia and School of Physics and Astronomy, University of Southampton, Highfield, Southampton SO17 1BJ, United Kingdom*

[2]*Science Institute, University of Iceland, Dunhagi-3, IS-107, Reykjavik, Iceland and Division of Physics and Applied Physics, Nanyang Technological University 637371, Singapore*

[3]*School of Physics and Astronomy, University of Southampton, Highfield, Southampton SO17 1BJ, United Kingdom*

[4]*Ioffe Physical-Technical Institute of RAS, 194021 St. Petersburg, Russia and Spin Optics Laboratory, St. Petersburg State University, 1, Ulianovskaya, 198504, Russia*

(Received 19 January 2012; published 7 May 2012)

Vertical cavity surface emitting terahertz lasers can be realized in conventional semiconductor microcavities with embedded quantum wells in the strong coupling regime. The cavity is to be pumped optically at half the frequency of the $2p$ exciton state. Once a threshold population of $2p$ excitons is achieved, a stimulated terahertz transition populates the lower exciton-polariton branch, and the cavity starts emitting laser light both in the optical and terahertz ranges. The lasing threshold is sensitive to the statistics of photons of the pumping light.

DOI: 10.1103/PhysRevLett.108.197401 PACS numbers: 78.67.Pt, 78.45.+h, 78.66.Fd

Creation of efficient sources of terahertz (THz) radiation is of high importance for various fields of modern technology, including information transfer, biosensing, security, and others [1]. These applications are currently limited due to the lack of compact and reliable solid state sources of THz radiation. The main obstacle preventing the creation of such a source is the low rate of spontaneous emission of THz photons: according to Fermi's ''golden rule'' this rate is proportional to the cube of the frequency and for THz transitions should be roughly tens of inverse milliseconds, while lifetimes of crystal excitations typically lie in the picosecond range [2,3]. The attempted strategies to improve this ratio include using the Purcell effect [4,5] by embedding the sample inside a THz cavity, or using the cascade effect in quantum cascade lasers [6] (QCLs). Nevertheless, until now QCLs in the spectral region around 1 THz remain costly, have macroscopic dimensions, are short-lived, and still show a quantum efficiency of less than 1%.

Recently, it has been proposed that the emission rate of THz photons may be increased by bosonic stimulation if the THz transition feeds a condensate of exciton-polaritons. In Refs. [7–9] the authors suggest using the transition between the upper and lower polariton branches in a semiconductor microcavity in the polariton lasing regime. The radiative transition between two polariton modes, accompanied by emission of a THz photon, may become allowed if an electric field mixing polariton and dark exciton states is applied to the cavity. THz photons would be emitted in the plane of the cavity, and a supplementary lateral THz cavity would be needed to provide the positive feedback.

Here we propose an alternative model of a microcavity based THz laser, which has significant advantages compared to one based on the transition between two polariton branches. We propose using two-photon pumping of a $2p$ exciton state, as has been realized already in GaAs based quantum well structures [10,11]. The direct transition to or from the $2p$ exciton state with emission or absorption of a single photon is forbidden by optical selection rules. Instead, a $2p$ exciton can radiatively decay to the lower exciton-polariton mode formed by the $1s$ exciton and cavity photon. This transition is accompanied by emission of a THz photon [12]. The inverse process (THz absorption by a lower polariton mode with excitation of a $2p$ exciton) has been recently observed experimentally [13]. The THz transition from the $2p$ state pumps the lowest energy exciton-polariton state, which eventually leads to the polariton lasing effect, widely discussed in the literature [14]. A macroscopic occupation of the lowest energy polariton state stimulates emission of THz photons so that, in the polariton lasing regime, the cavity would emit one THz photon for each optical photon emitted by the polariton laser, ideally.

The design of the laser and the involved energy levels are illustrated schematically in Fig. 1. This design has two crucial advantages with respect to that previously considered [7]: it allows for operation with an optically allowed THz transition, and it provides vertical emission of THz photons. The whole structure is microscopic; no waveguides or THz cavities are needed. This latter point is also a significant advantage with respect to the quantum cascade laser, which operates in the waveguide geometry. Moreover, the suggested scheme is very interesting from a fundamental point of view since, as shown below, the threshold of the proposed laser appears to be sensitive to the statistics of photons of the pumping light. Here we present the quantum model of this laser based on the Liouville equation for the density matrix describing the $2p$ exciton state, the lower polariton mode, and optical and THz photons.

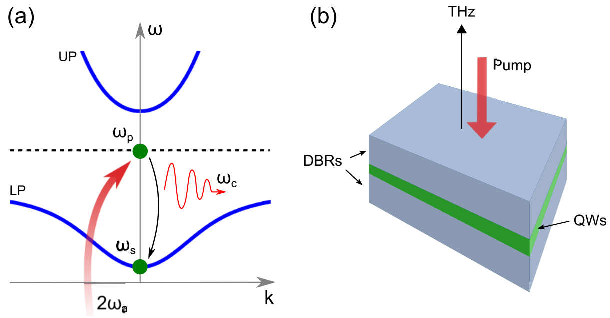

FIG. 1 (color online). (a) Schematic of the polariton dispersion relation, showing the lower-polariton (LP) and upper-polariton (UP) branches, as well as the $2p$ exciton state with frequency ω_p. The pump frequency, ω_a, is half that of the $2p$ exciton state, as discussed in the text. (b) The structure considered in this work: a semiconductor microcavity consisting of an active layer containing quantum wells (QWs) sandwiched between two distributed Bragg reflectors (DBRs). The structure is pumped vertically, i.e., in the direction perpendicular to the microcavity plane, and the resulting THz emission from the cavity is in the same direction.

The system under study consists of $2p$ excitons and $1s$ exciton-polaritons interacting with an external electromagnetic field and phonons in a semiconductor microcavity. Hence, our consideration involves both coherent and incoherent processes. Consequently, it is convenient to split the total Hamiltonian of the system into two parts,

$$H = H_c + H_d, \tag{1}$$

where the part H_c includes all types of coherent processes in our system and part H_d describes the decoherence in the system due to exciton interactions with acoustic phonons, modeled as a classical reservoir [15,16].

The equation for the density matrix can be written in the following form:

$$\frac{d\varrho}{dt} = \frac{i}{\hbar}[\varrho, H_c] + \hat{L}\varrho,$$

where $\hat{L}$ is a Lindblad superoperator defined below. The incoherent part of the Hamiltonian can be divided into two parts, $H_d = \sum_i (H_i^+ + H_i^-)$, where H_i^+ creates an excitation in the quantum system (and thus annihilates an excitation in the classical reservoir), and H_i^-, conversely, annihilates an excitation in the quantum system and creates an excitation in the classical reservoir. The subscript index i numerates different types of decoherence processes in the system.

The Lindblad terms can be then written as [16,17]

$$\hat{L}\varrho = \frac{\delta(\Delta E)}{\hbar}\sum_i \{(H_i^+ \rho H_i^- + H_i^- \varrho H_i^+) - (H_i^+ H_i^- + H_i^- H_i^+)\varrho - \varrho(H_i^+ H_i^- + H_i^- H_i^+)\}, \tag{2}$$

where $\delta(\Delta E)$ accounts for energy conservation, and in realistic calculations should be taken as an average inverse broadening of the states in our system, $\delta(\Delta E) \rightarrow \zeta^{-1}$. In the particular system which we consider, the coherent and incoherent parts of the Hamiltonian can be written as

$$H_c = \epsilon_p p^+ p + \epsilon_s s^+ s + \epsilon_a a^+ a + \epsilon_T c^+ c, \tag{3}$$

$$H_d = \sum_{i=1,2} (H_i^+ + H_i^-), \tag{4}$$

where

$$H_1^+ = g p^+ a^2, \tag{5}$$

$$H_1^- = g p a^{+2}, \tag{6}$$

$$H_2^+ = G p^+ s c, \tag{7}$$

$$H_2^- = G p s^+ c^+. \tag{8}$$

Here p and s denote annihilation operators of the $2p$ exciton and the lowest energy $1s$ polariton states, respectively; a is the annihilation operator for laser photons exciting the $2p$ exciton state; and c is an annihilation operator for THz photons produced by the $2p \rightarrow 1s$ transition. ϵ_p, ϵ_s, ϵ_a, and ϵ_T are the energies of the $2p$ exciton, $1s$ exciton-polariton, pump photon ($2\epsilon_a = \epsilon_p$) and THz photon, $\epsilon_T = \epsilon_p - \epsilon_s$, respectively. Constants g and G define the strengths of the two-photon absorption and $1s \rightarrow 2p$ radiative transitions, respectively. While the $1s \rightarrow 2p$ transition strength is determined by the dipole matrix elements, the main contribution to the two-photon $2p$ excitation comes from processes with intermediate states in the valence or conduction bands [18]. We assume that the upper polariton state is higher in energy than the $2p$ exciton state, and thus can be excluded from consideration. The classical reservoir consists of the photons of the external laser light and THz photons. Note that the coherent part of our Hamiltonian describes only the free modes of the system and thus is irrelevant to the kinetic equations.

Now, for the occupancy of the $2p$ exciton mode one can obtain after straightforward algebra

$$\frac{dN_p}{dt} = \mathrm{Tr}\left\{p^+ p \frac{d\varrho}{dt}\right\} = \frac{2}{\hbar\zeta}\mathrm{Re}\{\mathrm{Tr}(\varrho[H^-;[p^+p;H^+]])\} = W_g\left[\frac{1}{2}\langle a^{+2}a^2\rangle - \langle p^+p(2a^+a+1)\rangle\right] + W_G[\langle s^+ s c^+ c\rangle - \langle p^+ p(s^+ s + c^+ c + 1)\rangle], \tag{9}$$

where $\langle \ldots \rangle = \mathrm{Tr}\{\ldots \varrho\}$ denotes averaging with the appropriate density matrix ϱ, $W_g = 4g^2/\hbar\zeta$ and $W_G = 2G^2/\hbar\zeta$. The equations for the polariton mode occupancy $N_s = \langle s^+ s\rangle$, and the terahertz mode occupancy $N_c = \langle c^+ c\rangle$ are analogous to those for N_p. The occupancy of the pumping mode $N_a = \langle a^+ a\rangle$ is defined by the intensity of the external pump and we do not need to write an independent dynamic equation for it. The same holds true for the higher order correlators involving pump operators, e.g., $\langle a^{+2}a^2\rangle$. It follows from Eq. (9) that the dynamic equations for the occupancies of the modes contain quantum correlators of fourth order, such as $\langle s^+sc^+c\rangle$. For them one can also write the dynamic equations analogous to Eq. (9), which would contain correlators of sixth order. Proceeding further, one would obtain an infinite chain of coupled equations for the hierarchy of correlators.

In order to solve this chain of equations one needs to truncate the correlators at some stage. Here we use the mean-field approximation, which consists in truncation of the fourth-order correlators into products of second-order ones. One can approximate $\langle p^+pa^+a\rangle \approx \langle p^+p\rangle\langle a^+a\rangle = N_pN_a$, $\langle s^+sc^+c\rangle \approx N_sN_c, \ldots$, etc.

A particular analysis is needed for the truncation of the correlator $\langle a^{+2}a^2\rangle$ containing four operators corresponding to the pumping mode. Using the definition of the second order coherence $g^{(2)}(0)$, it can be represented as

$$\langle a^{+2}a^2\rangle = g^{(2)}(0)N_a^2. \tag{10}$$

Finally, the closed set of equations of motion describing the dynamics of our system reads

$$\frac{dN_p}{dt} = -\frac{N_p}{\tau_p} + W_g\left[\frac{g^{(2)}(0)}{2}N_a^2 - N_p(2N_a+1)\right] + W_G\{N_sN_c(N_p+1) - N_p(N_s+1)(N_c+1)\}, \tag{11}$$

$$\frac{dN_s}{dt} = -\frac{N_s}{\tau_s} - W_G\{N_sN_c(N_p+1) - N_p(N_s+1)(N_c+1)\}, \tag{12}$$

$$\frac{dN_c}{dt} = -\frac{N_c}{\tau_c} - W_G\{N_sN_c(N_p+1) - N_p(N_s+1)(N_c+1)\}, \tag{13}$$

where we have introduced the nonradiative lifetime of the $2p$ exciton state, τ_p, and lifetimes of lower polaritons and THz photons, τ_s and τ_c, respectively.

Let us analyze in more detail the kinetic equation for the $2p$ state occupation N_p. The terms describing incoming and outcoming scattering rates for this state can be written as

$$(1+N_p)\langle a^{+2}a^2\rangle - N_p\langle a^2a^{+2}\rangle.$$

As we already mentioned in Eq. (10), the incoming rate is proportional to $g^{(2)}(0)N_a^2$. The outgoing rate can be recast as $\propto \langle a^2(a^+)^2\rangle = g^{(2)}(0)N_a^2 + 4N_a + 2$. Hence, all terms containing $N_a^2N_p$ cancel each other and Eq. (11) holds. Note that for processes of nondegenerate two-photon absorption or emission neglected here, two-photon emission processes where photon frequencies are different can be included in τ_p, the decay rate of the $2p$ state. The scattering rates have standard form $(1+N_p)N_{a_1}N_{a_2} - N_p(N_{a_1}+1)(N_{a_2}+1)$, independent of the photon field statistics [19]. In what follows we assume that $N_a \gg 1$ making it possible to neglect all other modes.

The key feature of Eq. (11) is that the pumping term $W_gg^{(2)}(0)N_a^2$ contains the second order coherence of the pump, i.e., it strongly depends on its statistics. For a laser pump corresponding to the coherent state this statistics is Poissonian and $g^{(2)}(0) = 1$. On the other hand different radiation sources may provide different statistics of pump photons and different values of $g^{(2)}(0)$. For example, for a thermal pump $g^{(2)}(0) = 2$. Different values of $g^{(2)}(0)$ lead to the different lasing thresholds in the system. Note that dependence of two-photon optical processes on the second order coherence of light has been discussed by Ivchenko in Ref. [20]. In Fig. 2, we plot the steady state solutions for N_p and N_s, assuming that the terahertz mode occupation N_c is zero, for the cases of coherent and thermal pumps. For a qualitative understanding, we note that the threshold is reached if $N_s \sim 1$, or equivalently when $N_p \sim 1/\tau_sW_G$, since this signals the onset of Bose stimulation of the transition from the $2p$ state to the lower polariton, accompanied by terahertz emission. The terahertz generation rate is given by $T = W_GN_p(N_s+1) \approx 1/\tau_sN_s$, and therefore shows the same threshold behavior with pumping intensity as N_s, as can also be seen in Fig. 2. We observe that the threshold is higher in the case of a coherent pump, which may be understood in terms of the enhanced losses from the $2p$ state due to stimulated two-photon emission.

The dynamics of switching the system to polariton and terahertz lasing is essentially governed by the dynamics of the correlator $\langle a^{+2}a^2\rangle$, i.e., by the product of squared

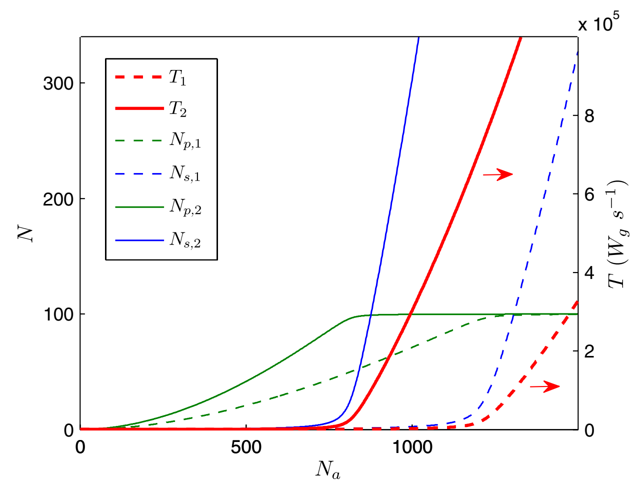

FIG. 2 (color online). Occupation of the p and s states in the steady state (left axis) and terahertz generation rate (right axis), as a function of pumping mode occupancy. The subscript 1 or 2 refers to the value of $g^{(2)}(0)$ taken. $W_g = 1$, $W_G = 10$, $1/\tau_s = 1000$, $1/\tau_p = 5000$, in units of W_g.

intensity and second order coherence of the pumping light. The efficiency of two-photon absorption W_g and the $1s$ polariton lifetime τ_s, dependent on the quality factor of the optical cavity, are two main factors which govern the threshold to lasing. The polarization of pumping defines the polarization of emission, and the frequency of THz radiation may be tuned by changing the exciton-photon detuning in the microcavity. Interestingly, THz lasing in our system is possible in the absence of a THz cavity. In order to demonstrate this, we have taken the terahertz photon lifetime $\tau_c = 0$ in the calculation shown in Fig. 2. One can see that THz lasing begins simultaneously with polariton lasing. The stimulated emission of THz photons is achieved due to the bosonic stimulation of this transition by occupation of the final ($1s$ polariton) state. The system emits THz radiation through the Bragg mirrors of the microcavity, which are transparent at THz frequencies.

In conclusion, we have developed a quantum theory of vertical cavity surface emitting terahertz lasers. The vertical terahertz lasing coexists with polariton lasing and, consequently, is characterised by a low pumping threshold. Interestingly, the value of the threshold is strongly dependent on the statistics of photons of the pumping light. For practical realization of compact terahertz lasers operating at room temperature, microcavities based on wide band gap semiconductors (GaN or ZnO) would seem to be the most advantageous. The resonant two-photon pumping of $2p$ exciton states in such a cavity may be assured by a conventional vertical cavity light emitting diode (VCLED) emitting in red. This prospective structure would consist of a GaN or ZnO microcavity grown on the top of a GaAs based VCLED structure. As emission of coherent terahertz light coexists with the polariton lasing in the optical frequency range in this scheme, one can use the visible blue or green light produced by the polariton laser as a marker for the terahertz light beam, which may be important for applications in medicine, security control, etc.

A. V. K. thanks Alberto Bramati, Elisabeth Giacobino, Elena Del Valle, and Fabrice Laussy for fruitful discussions, and M. M. G. is grateful to Alexander Poddubny for useful comments. This work has been supported by the visitors program of the International Institute of Physics (Natal, Brazil), and EU IRSES project "POLAPHEN." I. A. S. acknowledges support from Rannis "Center of Excellence in Polaritonics" and EU IRSES project "POLATER." M. M. G. was partially supported by RFBR.

[1] D. Dragoman and M. Dragoman, Prog. Quantum Electron. **28**, 1 (2004).
[2] H. T. Duc, Q. T. Vu, T. Meier, H. Haug, and S. W. Koch, Phys. Rev. B **74**, 165328 (2006).
[3] T. D. Doan, H. T. Cao, D. B. Tran Thoai, and H. Haug, Phys. Rev. B **72**, 085301 (2005).
[4] J.-M. Gerard and B. Gayral, J. Lightwave Technol. **17**, 2089 (1999).
[5] Y. Todorov, I. Sagnes, I. Abram, and C. Minot, Phys. Rev. Lett. **99**, 223603 (2007).
[6] R. F. Kazarinov and R. A. Suris, Sov. Phys. Semicond. **5**, 707 (1971); J. Faist, F. Capasso, D. L. Sivco, C. Sirtori, A. L. Hutchinson, and A. Y. Cho, Science **264**, 553 (1994); E. Normand and I. Howieson, Laser Focus World **43**, 90 (2007).
[7] K. V. Kavokin, M. A. Kaliteevski, R. A. Abram, A. V. Kavokin, S. Sharkova, and I. A. Shelykh, Appl. Phys. Lett. **97**, 201111 (2010).
[8] I. G. Savenko, I. A. Shelykh, and M. A. Kaliteevski, Phys. Rev. Lett. **107**, 027401 (2011).
[9] E. del Valle and A. V. Kavokin, Phys. Rev. B **83**, 193303 (2011).
[10] I. M. Catalano, A. Cingolani, R. Cingolani, M. Lepore, and K. Ploog, Phys. Rev. B **40**, 1312 (1989).
[11] R. A. Kaindl, D. Hagele, M. A. Carnahan, and D. S. Chemla, Phys. Rev. B **79**, 045320 (2009).
[12] N. Garro, S. P. Kennedy, A. P. Heberle, R. T. Phillips, Phys. Status Solidi (b) **221**, 385 (2000).
[13] J. Tomaino, A. Jameson, Y. Lee, G. Khitrova, H. Gibbs, A. Klettke, M. Kira, and S. Koch, arXiv:1112.2185.
[14] See, e.g., S. Christopoulos, G. Baldassarri Hoger von Hogersthal, A. Grundy, P. G. Lagoudakis, A. V. Kavokin, J. J. Baumberg, G. Christmann, R. Butte, E. Feltin, J. F. Carlin, and N. Grandjean, Phys. Rev. Lett. **98**, 126405 (2007); A. Das, J. Heo, M. Jankowski, W. Guo, L. Zhang, H. Deng, and P. Bhattacharya, Phys. Rev. Lett. **107**, 066405 (2011).
[15] E. B. Magnusson, H. Flayac, G. Malpuech, and I. A. Shelykh, Phys. Rev. B **82**, 195312 (2010).
[16] I. G. Savenko, E. B. Magnusson, and I. A. Shelykh, Phys. Rev. B **83**, 165316 (2011).
[17] T. Ostatnicky, I. A. Shelykh, and A. V. Kavokin, Phys. Rev. B **81**, 125319 (2010).
[18] E. L. Ivchenko and G. E. Pikus, *Superlattices and Other Heterostructures* (Springer-Verlag, Berlin, 1997).
[19] N. A. Enaki and O. B. Prepelitsa, Theor. Math. Phys. **88**, 967 (1991).
[20] E. L. Ivchenko, *Optical Spectroscopy of Semiconductor Nanostructures* (Alpha Science, Harrow, United Kingdom, 2005).